ABLE: Development of an Airborne Lidar

GIORGIO FIOCCO, PAOLO G. CALISSE, MARCO CACCIANI, STEFANO CASADIO, GIANDOMENICO PACE, AND DANIELE FUA*

Physics Department, University of Rome, Rome, Italy

31 December 1997 and 10 August 1998

ABSTRACT

The acronym ABLE (Airborne Lidar Experiment) identifies a project to develop and fly an optical radar on a stratospheric platform for studies related to atmospheric radiation and composition. The prototype, ABLE 1, has been successfully flown on board the M55 Geophysica aircraft in the Arctic campaign of December 1996–January 1997 to observe stratospheric clouds and aerosol. The lidar, which runs automatically, has been installed in the unpressurized bay of the aircraft where the temperature approaches the low values of external air. The lidar transmitter is based on a Nd:YAG laser, with second and third harmonic outputs. The receiver consists of a 0.3-m Cassegrain telescope and several detection channels to look at different wavelengths and polarizations. A fluid circulation unit connected to the aircraft provides heating control. The instrument can point to the zenith or to the nadir. In the past campaign only $\lambda = 532$ nm was utilized: observations were carried out at two polarizations, pointing to the zenith. The present status of the device and foreseeable developments are described.

1. Introduction

Lidars are powerful tools for remote sensing of aerosol and cloud properties as well as other atmospheric parameters. While most of the experience in their use was gained with ground-based systems, generally set up to provide profiles of the observable quantities on the vertical of the site, operating a lidar from an aircraft offers the capability to explore vast portions of space and observe phenomena where they are expected to occur. The upper troposphere and lower stratosphere are regions of considerable current interest since the condensation of volatile species has effects on the ozone layer and to the radiative budget. Because of the small number of high-altitude aircraft available to the scientific community, the difficult environmental conditions, and the limitations of size and weight, only a limited number of dedicated lidar systems appear to have so far been developed, essentially at the National Aeronautic and Space Administration's Goddard Space Flight Center, and flown on the WB-57F and ER-2 aircraft (see, e.g., Spinhirne et al. 1982; Alejandro et al. 1995; Jensen et al. 1996).

Specific utilization of lidars addresses a number of current problems. In the polar regions the observation of polar stratospheric clouds (PSCs) constitutes an interesting target, due to the heterogeneous chemistry occurring at their surface and the related denitrification. In the Tropics, the phenomenology connected to the Hadley cell, the cold tropopause region, and the relatively frequent disturbance caused by convective systems suggests that possible similarities with the chemistry occurring in polar regions may exist. At all latitudes the climatology of thin cirrus clouds is a matter of current interest. In the polar as well as in the tropical regions, difficult logistics play in favor of using lidars on high altitude aircraft.

In a basic configuration, a lidar provides backscattering profiles of aerosol layers and thin clouds by the elastic scattering technique. By using different wavelengths and polarizations, information on the composition and on the size and shape of particles is obtained. It is a task of current design to accommodate echoes at short and far distances, to overcome the problems of limited dynamic range and saturation generally present in the Rayleigh/Mie channels, and to enhance the sensitivity required for the Raman and differential absorption lidar (DIAL) channels.

2. Instrumental description: Generalities

The Airborne Lidar Experiment (ABLE) is a completely automated, medium-power lidar capable of operating in an unpressurized, cold environment such as that of a balloon or a stratospheric aircraft. The lidar,

* Additional affiliation: CNR Istituto di Fisica dell'Atmosfera, Frascati, Italy.

Corresponding author address: Dr. G. Fiocco, Dipartmento Di Fisica, Universita degli Studi di Roma, La Sapienza Piazzale Aldo Moro, 2, I-00185 Rome, Italy.

TABLE 1. Mechanical and electrical characteristics of the ABLE system.

External maximum dimensions	1852 l × 960 w × 800 h mm^3
Weight	350 kg
Power	600 W (laser)
	200 W (electronics, pumps)
Operating temperature range	approx. −80° to +30°C

designed to be installed on a Miasyschev M-55 aircraft, consists of a number of subsystems broadly identified as follows: the laser, the receiving telescope, the optics for directing the beams, the detectors and associated optics, the electronics including the computers, and the temperature control subsystem. The laser is a single-stage Nd:YAG unit with second and, if required, third harmonic generation. The receiver is based on a 0.3-m-diameter Cassegrain telescope followed by collimating optics, beam splitters, filters, and detectors. The telescope axis is horizontal, aligned with the aircraft longitudinal axis; the transmitted beam is rendered coaxial to it. Both beams can be directed for observation to the zenith or to the nadir by mirrors set at 45° to the telescope axis. The main subsystems are installed in separate boxes.

For its operation the lidar requires the following essential provisions from the aircraft: about 800 W, 27 V DC power and a thermally stabilized fluid for temperature control. Table 1 summarizes the main characteristics of the lidar referring to installation.

During the Arctic campaign of 1996–97 only zenith observations at $\lambda = 532$ nm in two polarizations were carried out. With the aircraft flying at the altitude of approximately 20 km, successful retrieval of profiles of the aerosol and molecular backscattering was demonstrated up to 30 km with 10 s of integration.

As platforms for optical observation, aircraft have general limitations due to turbulence and vibration. Operating the lidar on an unpressurized stratospheric aircraft requires additional attention in the development and in the operational phase: the related problems lead to the following key points, which have to be harmonized with the requirements on size, weight, power, and access.

The change in ambient pressure determines the necessity to house sensitive instrumentation in pressurized enclosures. The rapid variations of temperature, humidity, and pressure outside the aircraft result in variable conditions inside the bay where the lidar is installed. The generally lagging and nonuniform response of structures and enclosures is the cause of temperature gradients, stress, and deformations with consequences on the stability of the optical alignment. Changes in temperature and relative humidity may lead to condensation on optical surfaces. The sequence of events and the ensuing requirements may be quite different in the takeoff and in the landing phase, in the polar regions, and in the Tropics.

3. Aircraft modifications and connections between aircraft and lidar

a. The aircraft

The modified version of the M-55 stratospheric aircraft Geophysica can reach a ceiling altitude of about 21 km, taking off, if necessary, from poorly equipped airports, with no particular limitations posed by weather in comparison to similar airplanes. Among the features of direct impact on the operation of scientific equipment we should mention the relatively large payload capacity and available electric power, and the existence of a subsidiary thermal control unit capable of handling the lidar requirements.

The installation of ABLE required a few structural modifications, including the provision of windows for observation, the implementation of the subsidiary thermal control unit, and of an additional electric power generator, both devices dedicated to the lidar. All these modifications were carried out by the Myasischev Design Bureau, according to the instrumental requirements.

b. Structural modifications and lidar installation

With regard to the structural modifications, the aircraft larger bay, located in the lower section of the fuselage, has been subdivided to allow for the installation of different instruments (Stefanutti et al. 1998). The lidar has been installed in the forward section of the bay closest to the bow of the aircraft, below and forward of the cockpit. To access the instruments, during hangar operations, a cowling covering the entire bay can be removed. This operation requires approximately a half-hour and is not allowed outside of the hangar. During preflight conditions, limited access is available by an approximately 1-m-long hatch on the left side of the cowling.

The lidar is suspended to the aircraft structure through four dampers. To permit observations, two 300-mm diameter silica windows, aligned on the same vertical axis, were installed respectively on the upper and lower external surface of the fuselage. The directing optics (consisting as said of a coupled set of mirrors at 45°) located at the intersection between such axis and the horizontal axis of the receiving telescope, deviate the beams toward either window. The window facing the zenith is located approximately 2 m in front of the cockpit; the window glass leans forward by about 5° with respect to the horizontal plane, partially in accord with the aircraft aerodynamics, and to limit the effects of light reflections at its surface. The other window is placed on the cowling. Forward and side scanning geometries have been considered and might be implemented in the future.

c. The aircraft subsidiary thermal control system and electrical connections

The subsidiary thermal control unit, handling the heat exchange between the lidar and the aircraft, is located

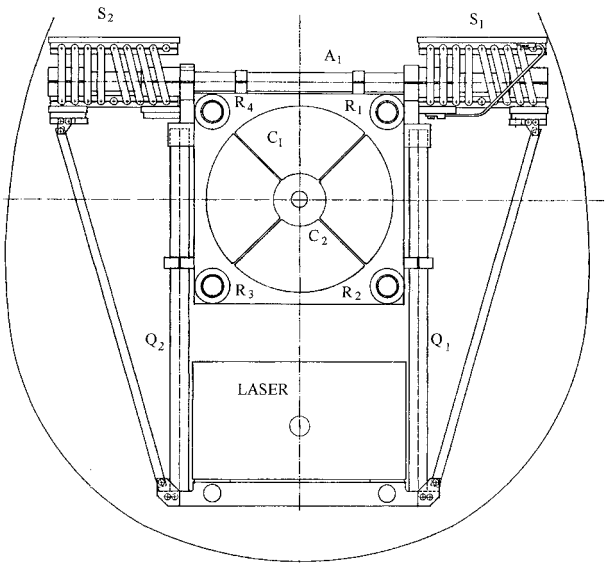

FIG. 1. Cross section of the lidar facing the Cassegrain telescope. (C) Cassegrain telescope mirrors, (S) mechanical dampers, (a) transverse rods, (r) longitudinal rods, and (q) vertical rods.

in a different section of the aircraft. This unit controls the temperature of a circulating fluid (diluted glycol) by modulating the heat transfer: the unit includes an air-to-liquid heat exchanger, dissipating excess heat to the external air, a flow regulator, electric heaters, and temperature sensors, and is connected via two heat exchangers to the lidar circuits.

The ABLE total electrical power consumption is approximately 800 W, 600 W being used by the laser. To provide the laser power, a dedicated 27 V DC–1 kW supply was installed in the aircraft, to avoid possible disturbances to the avionics and other instrumentation. The laser unit is, however, provided with adequate filters to quench undesirable interferences. Another supply, shared with other instruments, is used to power the other subsystems (electronics, computer, and pumps). Power at 110 V, 400 Hz is provided but not used at present.

Flight data can be acquired in real time from a dedicated unit in the aircraft, which converts and distributes flight parameters to any user through an RS-422 serial port. Two lamps in the cockpit, driven by the ABLE software, flash to signal the correct operation of the instrument to the pilot. The lidar can be switched on and off by the pilot; the pilot can also start and stop the laser beam emission for safety reasons, while leaving the rest of the lidar system running.

4. Details of the instrumental layout

a. Supporting structure

Basically, the instrument can be figured as a number of separate subsystems held together by a frame of light-alloy pipes and steel elements. Figures 1 and 2 display the construction plans of the system: front-end view and lateral view, respectively; some key elements are labelled with letters used in the description that follows. The main subsystems to be considered are the laser, the optics for directing the beams in and out of the aircraft, the receiving telescope, the detectors and the electronics, and the thermal control unit. The laser and the detectors–electronics are located, respectively, in two pressurized and thermally controlled boxes. The telescope and the directing optics are also configured as boxes.

The dampers, $S_{1,2,3,4}$, that connect the lidar to the aircraft are placed at the four vertices of a trapezoid and

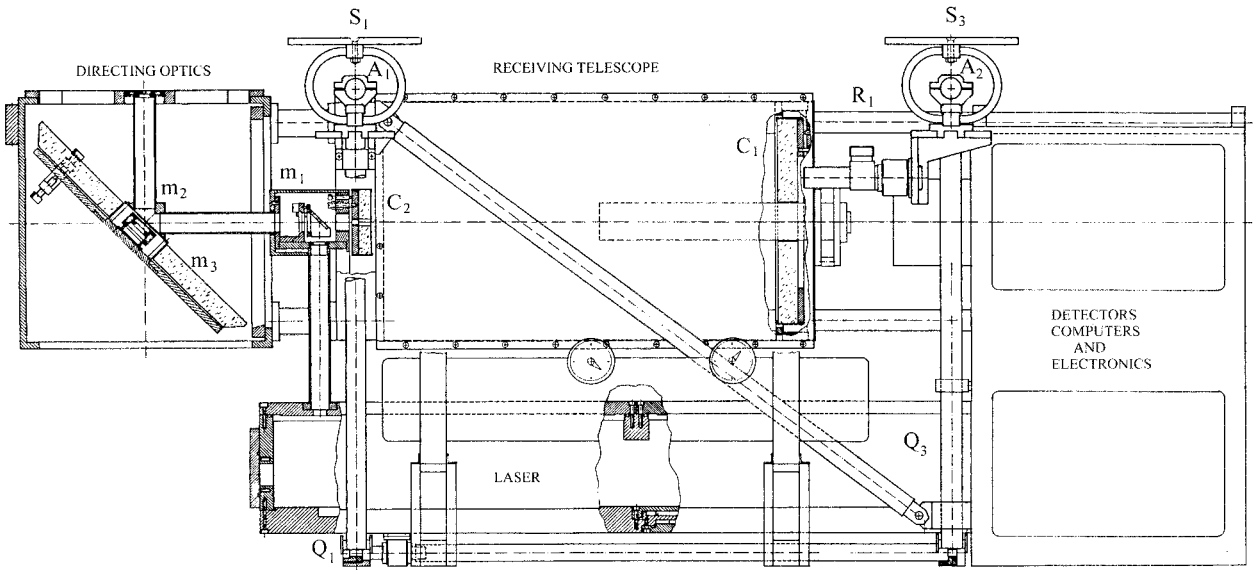

FIG. 2. Lateral view of the lidar. Elements are labeled as follows: (m) mirrors, (C) Cassegrain telescope mirrors, (R) longitudinal rods, (Q) vertical rods, (A) transverse rods, and (S) mechanical dampers.

TABLE 2. Characteristics of the Quanta System laser as used during the 1996–97 Arctic campaign.

Pulse energy	100 mJ
Wavelength	532 nm
Pulse duration	10 ns
Divergence	0.5 mrad without beam expander
Pulse rate	10 Hz
Power consumption	600 W

are clamped at the ends of two horizontal bars, $A_{1,2}$, which are part of the lidar frame. The bars are transverse to the aircraft longitudinal axis, at a mutual distance of 900 mm: due to the shape of the fuselage, they are of different length, the forward bar, 850 mm long, being shorter than the backward, 960 mm long. Two vertical tubes, Q, at a distance of 410 mm are attached to each bar: the four tubes essentially support all the structure. Four other tubes, $R_{1,2,3,4}$, are symmetrically positioned around the telescope, connecting its optical elements to the directing optics in front of the telescope and, in the upper part, to the detector box in the rear. Other tubular elements are mounted diagonally on the longitudinal and transverse planes to stiffen the frame.

The laser box (1050 l $\times$ 366 w $\times$ 200 h mm^3), lodged in the lower section of the instrument, rests on bearings that allow for small relative displacements of its front end, while the back is fixed, due to differential, thermal—and, possibly, pressure induced—expansion of the box, with no resulting misalignment of the laser beam.

The receiver box (410 l $\times$ 525 w $\times$ 670 h mm^3) is rigidly anchored to the supporting structure. Being pressurized, in flight the box undergoes a certain amount of deformation: efforts have been made to minimize its effects on the optical alignment.

The directing optics setup is mounted in a box, directly attached to the four longitudinal bars, $R_{1,2,3,4}$, that surround the Cassegrain telescope. This arrangement allows to rotate the unit and direct the beams in 90° steps in the plane transverse to the aircraft axis. This adjustment is carried out manually on the ground. A laboratory prototype of a motorized unit was constructed, which would allow redirecting and scanning the beams in flight.

b. Laser

The core of the lidar transmitter is a single stage Nd:YAG pulsed laser specially developed by Quanta System of Milan. The laser is equipped with second and third harmonic generators: in the Arctic flight the third harmonic was removed and only the second harmonic output ($\lambda = 532$ nm) was used, at a fixed repetition rate of 10 Hz. Table 2 summarizes its characteristics.

The laser consists of two sections: the power supply and the head, both housed in the same pressurized and thermally controlled box. The laser head consists of a resonator cavity, with Gaussian optics, that emits short ($\approx$10 ns), linearly polarized pulses at $\lambda = 1046$ nm with energy about 400 mJ; the repetition rate can be chosen between 1 and 10 Hz. The active medium is a Nd:YAG rod, pumped by a flashlamp. Heat is removed from the rod and flashlamp with a closed-loop distilled-water circulation. Two lenses correct for the distortion of the beam caused by the thermally induced deformations of the rod. The polarization of the beam is converted to circular by a quarter-wave plate before entering the second harmonic generator consisting of a temperature controlled KD*P crystal, used with type I angular phase matching, with a converting efficiency of about 40%. The pulses at 532 nm have an energy of about 150 mJ and are linearly polarized. The third harmonic generator can be installed next. Finally a dichroic mirror reflects at 90° the short-wave emissions vertically and out of the box through an antireflection coated glass window located in the top cover, while the infrared part is damped out. If required, the laser light can also exit from the front wall of the box. The laser head section contains the circuits for powering and timing the flashlamp, the Pockels cell, as well and the temperature control circuits for the harmonic generators. The bottom plate, which constitutes the basis of the box, incorporates a liquid–liquid heat exchanger where the cooling circuit of ABLE is interfaced to the laser own water circulation, also providing thermal stabilization of the entire box.

c. Transmitting, directing, receiving optics and detectors

Figure 3a displays a schematic diagram of the different parts of the system. After leaving the laser, the emitted beam may go through an optional, small two-lens telescope (t_1) to be expanded and if necessary increase its divergence for the purpose of eye safety. It then encounters a mirror (m_1), mounted on the backside of the secondary mirror of the Cassegrain telescope (C_2), which bends it at 90°, to make it, from now on, coaxial with the received beam. Both optical paths then encounter the mirrors, which constitute the directing optics setup.

This unit consists of two coplanar, concentric flat mirrors placed at 45° to the Cassegrain axis for the purpose of deflecting the outgoing beam and the received signal. The large mirror (m_3), facing the receiving telescope, is of ellipsoidal shape, with about 300-mm minor axis; its surface (A1 coated and SiO_2 protected) has a central hole to allow for the installation of the small mirror treated with a hard dielectric coating (m_2): it has not been considered feasible, due to the high power of the laser, to use a single mirror for both optical paths. In addition, the two beams have to be kept separated to limit as much as possible the amount of laser radiation scattered into the receiver within and near the instrument. It has not been considered so far feasible to install a rotating shutter to avoid short-range unwanted echoes and saturation. Reliance has been made on the distant

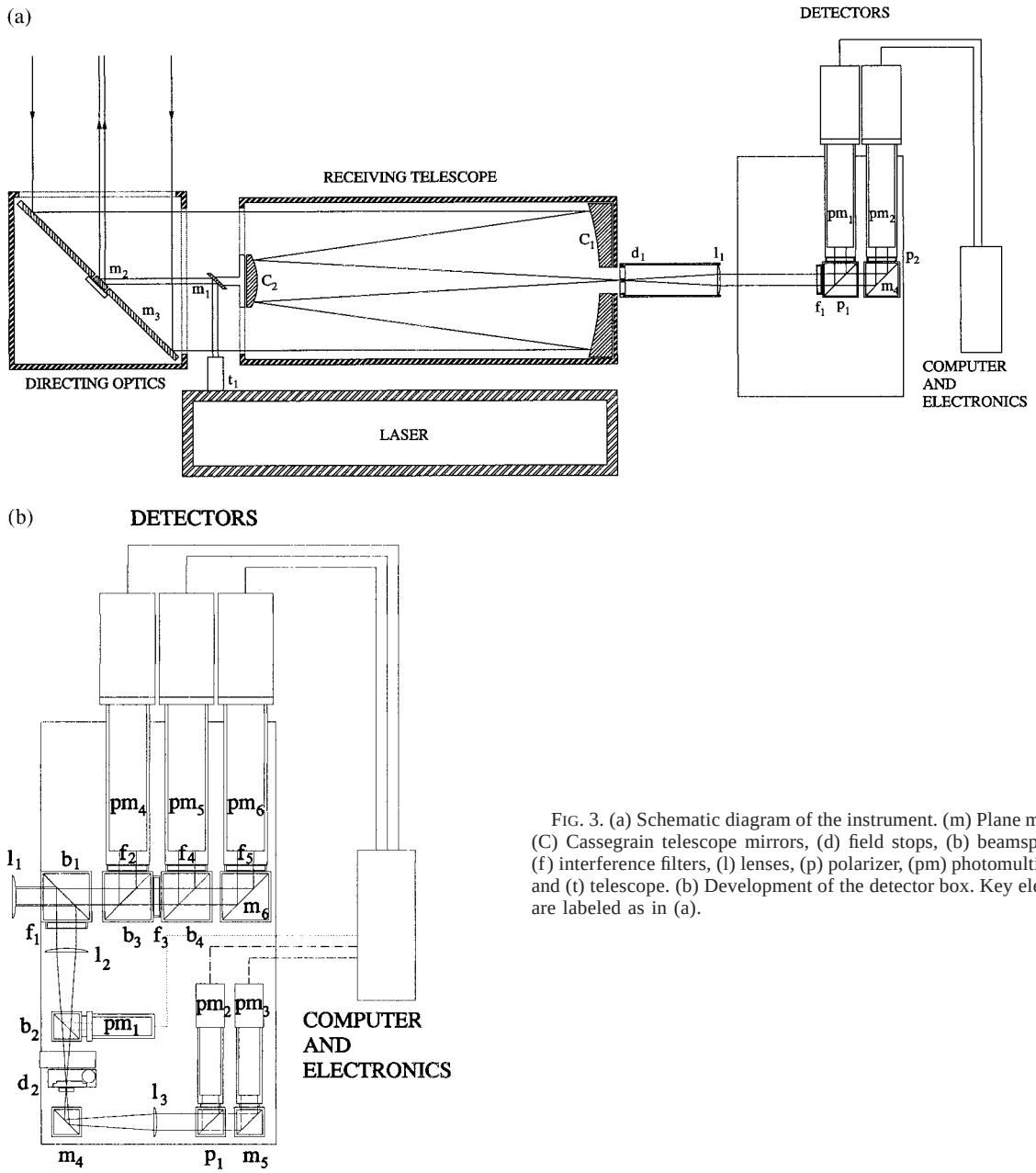

FIG. 3. (a) Schematic diagram of the instrument. (m) Plane mirrors, (C) Cassegrain telescope mirrors, (d) field stops, (b) beamsplitters, (f) interference filters, (l) lenses, (p) polarizer, (pm) photomultipliers, and (t) telescope. (b) Development of the detector box. Key elements are labeled as in (a).

overlap of the transmitted and received beams, on the precise alignment of the beams, on the shading produced by the Cassegrain secondary, and on accurate screening and control of the field of view.

The radiation backscattered from the atmosphere is collected by the Cassegrain telescope (see Table 3). The primary paraboloid (C_1) has a useful diameter of 300 mm and a focal ratio $f/3$; the combined focal ratio is $f/7.9$. An iris (d_1) on the focal plane followed by a manual shutter and by a collimating lens (l_1) limits the field of view. After this sequence of elements, the collimated received beam enters the pressurized detector box through a window.

TABLE 3. Characteristics of the receiving optics.

Combined length of the telescope	2234 mm (f/7.79)
Diameter of the primary mirror	300 mm
Focal length of the primary mirror	900 mm
Diameter of the secondary mirror	110 mm

Within the box, in the simplest configuration flown in the Arctic campaign, the beam went successively through an interference filter (f_1), a polarizing beam splitter (p_1), and then to two 14-stage Thorn EMI

9813QA photomultipliers (pm_1 and pm_2). After the photomultipliers the signals were amplified by a factor of 30 before entering the photon counting units. To reduce possible noise, lithium batteries were used in the detector section.

After the Arctic campaign the receiver development has been continued, to extend the range of distances covered, the dynamic range, the field of view, and the number of observed wavelengths. The present design shown in Fig. 3b aims at acquiring echoes at 532 nm in both polarizations from a distance beyond approximately 1 km, and echoes at 532 nm, 355 nm, and at two Raman wavelengths from shorter distances. For this purpose, after l_1, the radiation at 532 nm is deviated by a dichroic beam splitter b_1, sent through an interference filter f_1, refocused by l_2, and after diaphgram d_2, which limits the field of view to far distance echoes, recollimated by l_3. The parallel 532-nm beam is then sent to a polarizing beam splitter p_1 before ending up on the photomultipliers pm_2 and pm_3 for the two polarizations. A beam splitter located just before d_2 picks up a small fraction of the light received at 532 nm to permit retrieval of signals at short range. The light transmitted by b_1 goes through a cascade of beam splitters (b_3, b_4) and through interference filters (f_2, f_3, f_4, and f_5), which separate the elastic echoes at 355 nm from two channels to be used for O_2 and H_2O Raman echoes, or for DIAL observations. In this way it is possible, by slightly defocusing the receiving optics and by opening d_1, to extend the detectivity at short range and avoid saturation, while maintaining a narrow field of view at a distance.

d. Data acquisition and storage

During the Arctic campaign the amplified signals from the detectors were sent to two EG&G TurboMCS photon counting units. The basic counting interval was set to 0.5 μs, corresponding to a range resolution of 75 m, for a total range of 512 intervals equivalent to 38 400 m. Control of the various units, data acquisition, and storage was performed by a low consumption, small-sized PC/104 8088 computer. Data were integrated for 10 s, transferred to the computer, and then saved on a hard disk drive; the computer also stored some housekeeping parameters.

The current evolution of the instrument has led to an increase and diversification of the electronics for data acquisition including channels for photon counting and analog-to-digital conversion, and a second computer. A battery operated datalogger has been installed, providing an autonomous record of the temperature at various points and of the pressure, inside the detector box, and in the bay.

e. Thermal control

The environmental conditions to which the lidar may be subjected are very different. On the ground they are expected to range from the cold and dry climate of the polar regions to the warm and humid one of the equatorial regions; in flight, at a ceiling altitude of 21 km, corresponding to a pressure around 40 hPa, the external air temperature can reach values lower than -80°C. The change from ground to flight conditions is generally large and rapid. A detailed and reliable prediction, at all times of the flight, of the thermal conditions inside the unpressurized payload bay and on several critical elements, cannot be carried out easily and reliance has to be made on thermal control and use of insulation. In normal conditions heat is to be removed from the laser and the electronics, which are installed in closed boxes. Depending on thermal inertia, heat is to be supplied to various elements to avoid critical deformations, damage, and the condensation of water. Cold spots, ensuing condensation, and problems with high voltages may occur within a tight box unless flushing with inert gas, which would create additional practical problems, is carried out. During the descent phase, when humid air fills the bay, the still cool optical elements may become a site for condensation.

In the lidar, cooling, and, sometimes, heating of the various subunits is carried out in various stages and through different circuits. The aircraft subsidiary cooling unit provides a fluid that is maintained between approximately 9° and 15°C. This unit is connected to two exchangers in the lidar where the aircraft system exchanges heat with the glycol flowing in two separate intermediate circuits, respectively, dedicated to the laser and to the detector boxes.

In principle, when running in a cold environment, the lidar could operate without being connected to the thermal control system of the aircraft, since the heat produced by the laser and the electronics can be used to maintain the temperature of the various subsystems within working range. In the event of failure, however, such provision is essential in keeping the apparatus above a critical temperature and, in particular, to avoid freezing of the distilled water used in the laser head, with consequent substantial damage.

Besides, during preflight operations when the aircraft systems are not working, an auxilliary thermal control system is available on the ground.

5. Operational considerations and tests

a. Laser safety

Restrictive rules apply to laser operations in the open air. Two aspects of this problem were considered, namely, the disturbance to the pilot and eye safety for others. In the first case, considering that during zenith observations the laser beam is emitted in front of the cockpit, although in a direction orthogonal to the line of flight, consideration was given to possible disturbances to the pilot's eyesight arising, during flight and in darkness, from scattering by particles. A simulation was carried

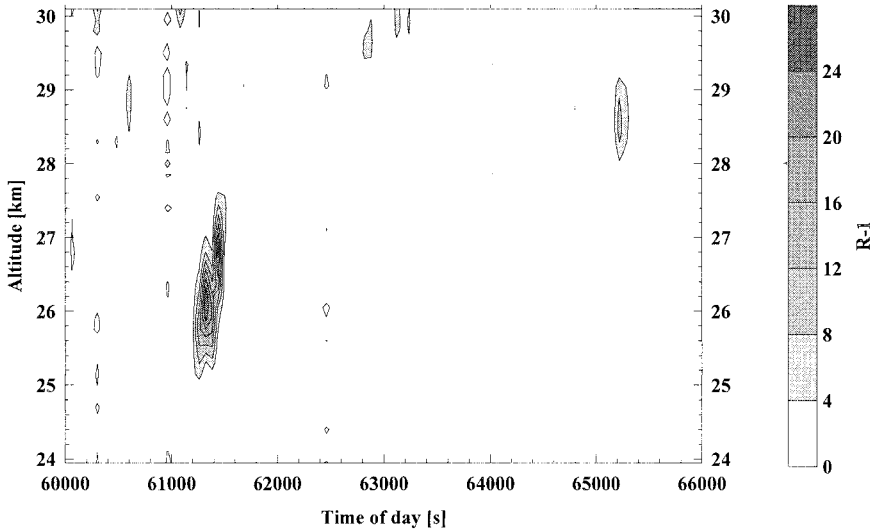

FIG. 4. Backscattering ratio $R - 1 = \beta_{aer}/\beta_{mol}$ at parallel polarization obtained in flight from Rovaniemi, Lapland, on 9 Jan 1997, showing the presence of polar stratospheric clouds.

out in the hangar at the Pratica di Mare airport, to measure the amount of radiation scattered in the worst conditions expected during flight. A transparent tube was placed on the lidar window, coaxially with the emitted beam, and an aerosol of variable number density and size was generated and allowed to flow in the pipe; with the lidar on, the total amount of radiation possibly collected by the eye's pupil was measured with a calibrated photodetector installed in the pilot's eye position. The detector sensitivity was 10^{-7} J cm^{-2} while the maximum permitted exposure (MPE) is 7.3×10^{-3} J cm^{-2} (American National Standard Institute 1993). The measured radiation was always below the sensitivity of the detector, showing that the maximum amount of radiation collected was within allowed limits.

In the nadir pointing case, using the working laser energy and divergence (Table 2), it can be shown that the energy density reaching the ground in clear-sky conditions is below the MPE value whenever the aircraft flies higher than 7000 m.

The probability that the beam emitted to the zenith might hit the eyes of an observer flying at higher altitude, although low, could not be neglected, especially during airport approach maneuvers. In general the existence of a ground-based lidar is notified to aviators by means of a NOTAM report. During the ABLE flights, the beam was switched on only at altitudes higher than 10 km.

b. Functional tests

A mechanical and hydraulic mock-up of the lidar was constructed: ground tests on the mock-up and on the actual system were performed to comply with RTCA-DO160C regulations that apply to airborne devices.

The reliability of the laser was checked in a first series of runs on a vibration table; the laser was operating and the emitted power measured during runs. No misalignments and no reduction on the laser output became evident after 2 h of vibrations on each axis.

A second series of tests were performed on the mock-up with vibration and shock tables, at 6*g* rms on each axis for 2 h: the mock-up was mechanically interfaced with the table by four steel dampers analogous to those mounted on the lidar. The dampers filter out more than 90% of the energy in the high frequency range. Successively the mock-up was installed on the M-55 and flown from Zukhovsky airport, in Russia, to check its behavior in real flight conditions.

Electromagnetic interference tests were also performed, in successive stages of the development, to check compliance with the RTCA-DO160C regulations.

Figure 4 shows results obtained during a flight from Rovaniemi: the data indicate the backscatter ratio, $R - 1 = \beta_{aer}/\beta_{mol}$, in the parallel polarization channel as a function of time and altitude above the aircraft. The obtained values clearly indicate the presence of polar stratospheric clouds at least in two distinct cases.

Acknowledgments. Financial support for the development of ABLE was provided in part by the Agenzia Spaziale Italiana and by Programma Nazionale Ricerche in Antartide. The competent collaboration of personnel of Myasischev Design Bureau and of the Italian Air Force at Pratica di Mare airport is acknowledged, as well as the support of ENEA for the environmental tests carried out at the Casaccia Laboratory. Thanks are also due to Antonio Febo for eye safety tests, to Giuseppe Puccetti for advice, and to Leopoldo Stefanutti for organizing the Airborne Polar Experiment.

REFERENCES

Alejandro, S. B., and Coauthors, 1995: Atlantic atmospheric aerosol studies 1. Program overview and airborne lidar. *J. Geophys. Res.*, **100,** 1035–1041.

American National Standard Institute, 1993: Laser safety measurements and instrumentation. Tech. Rep. ANSI Z136.1, 120 pp.

Jensen, E. J., O. B. Toon, H. B. Selkirk, J. D. Spinhirne, and M. R. Schoeberl, 1996: On the formation and persistence of subvisible cirrus clouds near the tropical tropopause. *J. Geophys. Res.*, **101,** 21 361–21 375.

Spinhirne, S. T., M. Z. Hansen and L. O. Caudill, 1982: Cloud top remote sensing by airborne lidar. *Appl. Opt.*, **22,** 1564–1571.

Stefanutti, L., A. R. MacKenzie, S. Balestri, V. Khattatov, G. Fiocco, E. Kyro, and Th. Peter, 1998: APE-POLECAT—Rationale, road map and summary of measurements. *J. Geophys. Res.*, in press.